Journal of Alloys and Compounds 504 (2010) 548–551

Contents lists available at ScienceDirect

Journal of Alloys and Compounds

journal homepage: www.elsevier.com/locate/jallcom

Rapid synthesis and consolidation of nanostructured $TaSi_2$–SiC–Si_3N_4 composite from mechanically activated powders by high-frequency induction-heated combustion

In-Yong Ko[a], Soo-Kyung Bae[a], Jin-Kook Yoon[b], In-Jin Shon[a,*]

[a] Division of Advanced Materials Engineering and the Research Center of Advanced Materials Development, Engineering College, Chonbuk National University, 664-14 Deokjin-dong 1-ga, Deokjin-gu, Jeonju, Jeonbuk 561-756, Republic of Korea
[b] Advanced Functional Materials Research Center, Korea Institute of Science and Technology, PO Box 131, Cheongryang, Seoul 130-650, Republic of Korea

ARTICLE INFO

Article history:
Received 4 March 2010
Received in revised form 18 May 2010
Accepted 1 June 2010
Available online 11 June 2010

Keywords:
Powder technology
Composite materials
Sintering
Nanomaterials
Mechanical properties

ABSTRACT

A dense nanostructured 5$TaSi_2$–SiC–Si_3N_4 composite was synthesized by the high-frequency induction-heated combustion synthesis (HFIHCS) method within 1 min in one step from mechanically activated powders of 4TaN, TaC and 14Si. Simultaneous combustion synthesis and densification were accomplished under the combined effects of the induced current and mechanical pressure. A highly dense 5$TaSi_2$–SiC–Si_3N_4 composite with relative density of up to 96% was produced under the simultaneous application of a pressure of 60 MPa and the induced current. The average grain size and mechanical properties (hardness and fracture toughness) of the composite were investigated.

1. Introduction

An increase in operating temperature of a gas turbine engine will bring us reductions in both fuel consumption and CO_2 emissions. It requires ultra-high temperature structural materials which overwhelm the performance of nickel-based superalloys commercially used as turbine blade and rotors. Among candidate materials based on refractory metal elements, refractory metal silicides have an attractive combination of properties, including high melting temperature, high modulus, high oxidation resistance in air, and a relatively low density [1,2]. However, as in the case of many intermetallic compounds, the current concern about these materials focuses on their low fracture toughness below the ductile-brittle transition temperature [3,4]. To improve their mechanical properties, the approach commonly utilized has been the addition of a second phase to form composites and to make nanostructured materials [5–10]. One example of this is the addition of Si_3N_4 and SiC to $TaSi_2$ to improve the latter's properties. Silicon nitride has a high thermal shock resistance, due to its low thermal expansion coefficient, and good resistance to oxidation when compared to other structural materials [11,12]. The isothermal oxidation resistance of the $NbSi_2$–40 vol.% Si_3N_4 composite prepared by the spark plasma sintering (SPS) process in dry air at 1300 °C was superior to that of monolithic $NbSi_2$ compact since the composite contained a larger amount of Si, which made it easier to form dense SiO_2 scale [13]. Also the addition of SiC had a significant influence on the behavior of $MoSi_2$, by forming a protective SiO_2 layer leading to its exhibiting outstanding oxidation resistance [14]. Therefore, Si_3N_4 and SiC may be the most promising additives for use as reinforcing material for $NbSi_2$-based composites.

As nanomaterials possess high strength, high hardness, excellent ductility and toughness, undoubtedly, more attention has been paid for the application of nanomaterials [15]. The grain size in sintered materials becomes much larger than that in pre-sintered powders due to a fast grain growth during conventional sintering process. Therefore, controlling grain growth during sintering is one of the keys to the commercial success of nanostructured materials. In this regard, the high-frequency induction-heated sintering method (HFIHSM), which can make dense materials within 2 min, has been shown to be effective in achieving not only rapid densification to near theoretical density but also the prohibition of grain growth in nanostructured materials [16,17].

The objective of this study is to investigate the preparation of a dense nanophase 5$TaSi_2$–SiC–Si_3N_4 composite by the high-frequency induction-heated combustion method starting from a mixture of mechanically activated TaN, TaC and Si powders.

* Corresponding author. Tel.: +82 63 270 2381; fax: +82 63 270 2386.
E-mail address: ijshon@chonbuk.ac.kr (I.-J. Shon).

0925-8388/$ – see front matter © 2010 Elsevier B.V. All rights reserved.
doi:10.1016/j.jallcom.2010.06.009

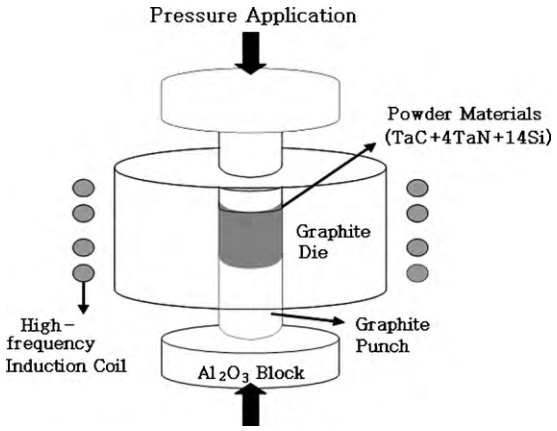

Fig. 1. Schematic diagram of the high-frequency induction-heated combustion apparatus.

2. Experimental procedure

Powders of 99.5% pure titanium nitride (−325 mesh, Alfa Products), 99.5% pure titanium carbide(−325 mesh, Cerac Products) and 99.5% pure silicon (−325 mesh, Aldrich Products) were used as the starting materials. Powder mixtures of TaN, TaC and Si in the molar proportion of 4:1:14 were first milled in a high-energy ball mill (Pulverisette-5, planetary mill) at 250 rpm for 10 h. Tungsten carbide balls (5 mm in diameter) were used in a sealed cylindrical stainless steel vial under an argon atmosphere. The weight ratio of ball to powder was 30:1. Milling resulted in a significant reduction of the grain size. The grain size and the internal strain were calculated by Suryanarayana and Grant Norton's formula [18]:

$$B_r(B_{crystalline} + B_{strain})\cos\theta = k\lambda/L + \eta\sin\theta \quad (1)$$

where B_r is the full width at half-maximum (FWHM) of the diffraction peak after instrument correction; $B_{crystalline}$ and B_{strain} are FWHM caused by small grain size and internal stress, respectively; k is constant (with a value of 0.9); λ is wavelength of the X-ray radiation; L and η are grain size and internal stress, respectively; and θ is the Bragg angle. The parameters B and B_r follow Cauchy's form with the relationship: $B = B_r + B_s$, where B and B_s are FWHM of the broadened Bragg peaks and the standard sample's Bragg peaks, respectively.

After milling, the mixed powders were placed in a graphite die (outside diameter, 45 mm; inside diameter, 20 mm; height, 40 mm) and then introduced into the high-frequency induction-heated combustion system as shown in Fig. 1. Following the introduction of the die into the apparatus, the system was evacuated and a uniaxial pressure of 60 MPa was applied. The induced current (with a frequency of about 50 kHz) was then activated and maintained until densification was attained as indicated by the linear gauge used to measure the shrinkage of the sample. The temperatures were measured by a pyrometer focused on the surface of the graphite die. At the end of the process, the sample was cooled to room temperature. The process was carried out under a vacuum of 40 mtorr.

The relative densities of the synthesized sample were measured by the Archimedes method. Microstructural characterization was performed on the product samples which had been polished and etched using a solution of HF (30 vol.%), HNO_3 (30 vol.%) and H_2O (40 vol.%) for 15 s at room temperature. Compositional and microstructural analyses of the products were conducted by X-ray diffraction (XRD) and scanning electron microscopy (SEM) in conjunction with energy dispersive X-ray analysis (EDAX). The Vickers hardness was measured by performing indentations at a load of 1 kg and a dwell time of 15 s.

3. Results and discussion

Fig. 2 shows XRD patterns of the raw powders and the milled 4TaN + TaC + 14Si powder mixture. The FWHM of the milled powder is greater than that of the raw powders, due to the internal strain and reduction in the grain size. The average grain sizes of the milled TaN, TaC and Si powders using Suryanarayana and Grant Norton's formula [18] were determined to be 21, 19 and 15 nm, respectively.

The interaction between these phases, i.e.,

$$4TaN + TaC + 14Si \rightarrow 5TaSi_2 + SiC + Si_3N_4 \quad (2)$$

is thermodynamically feasible.

The variations in the shrinkage displacement and temperature with the heating time during the processing of the 4TaN + TaC + 14Si system are shown in Fig. 3. As soon as the induced current was applied, the shrinkage displacement abruptly increased and, subsequently, the specimen initially showed a small amount of (thermal) expansion and the shrinkage displacement abruptly increased at about 1150 °C. When the reactant mixture of 4TaN + TaC + 14Si was heated to 1100 °C under a pressure of 60 MPa, no reaction took place as judged by the subsequent XRD analysis. The X-ray diffraction results, shown in Fig. 4a and b, exhibit only peaks pertaining

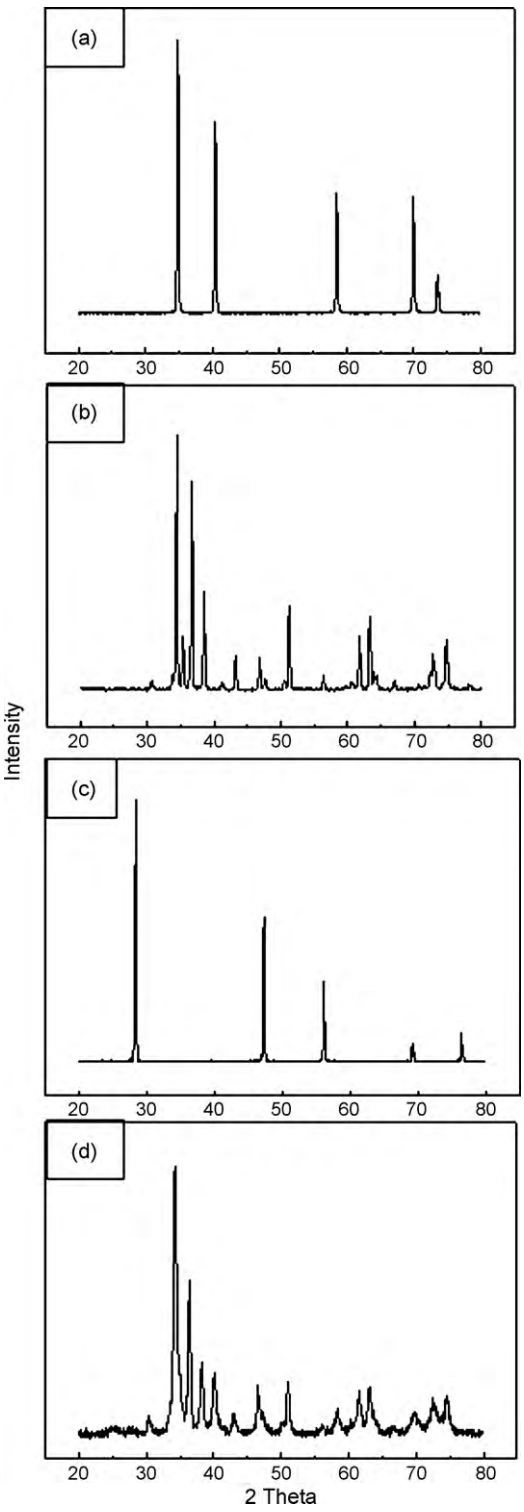

Fig. 2. XRD patterns of raw materials: (a) TaC, (b) TaN, (c) Si, and (d) milled TaC + 4TaN + 14Si.

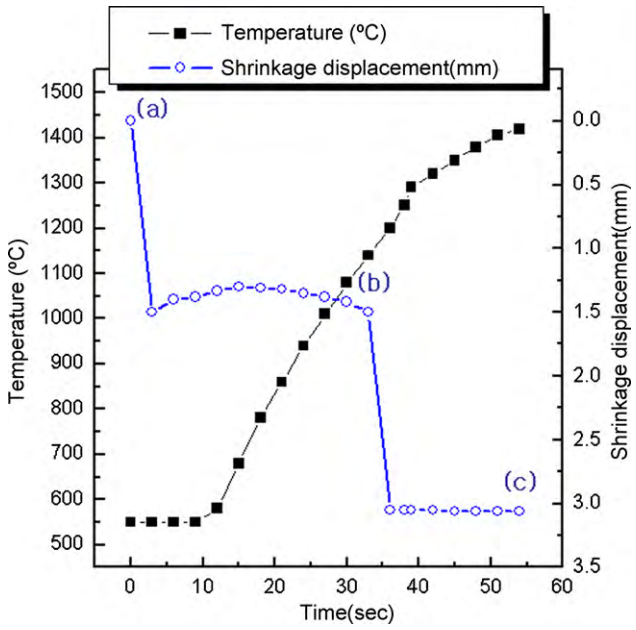

Fig. 3. Variations of temperature and shrinkage displacement with heating time during high-frequency induction-heated combustion synthesis and densification of $5TaSi_2$–SiC–Si_3N_4 composite (under 60 MPa, 90% of total output power capacity).

to the reactants TaN, TaC and Si. However, when the temperature was raised to 1420 °C, the starting powders reacted with each other producing products ($5TaSi_2$–SiC–Si_3N_4) as shown in Fig. 4c. Fig. 5a and b shows the SEM images of the powder after milling, and the sample heated to 1420 °C, respectively. Fig. 4a shows the presence of the reactants as separate phases. The SEM image of the etched surface of the samples heated to 1420 °C under a pressure of 60 MPa is shown in Fig. 5b. The grain boundary is not clear. So, The microstructure consists of nanograins observed by FE-SEM as shown in Fig. 6. The reaction between TaN, TaC and Si went to completion under these conditions. The X-ray diffraction analyses of this sample only showed peaks for $TaSi_2$, SiC and Si_3N_4, as indicated in Fig. 4c. The average grain sizes of $TaSi_2$, SiC and Si_3N_4 calculated by Suryanarayana and Grant Norton's formula [18] were about 35, 55 and 72 nm, respectively. And its corresponding density is approximately 5.89 g/cm^3 (relative density; 96%).

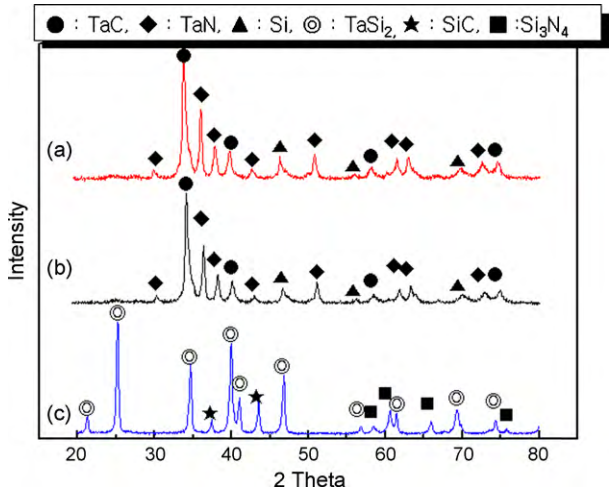

Fig. 4. XRD patterns of the TaC + 4TaN + 14Si system: (a) after milling, (b) before combustion synthesis, and (c) after combustion synthesis.

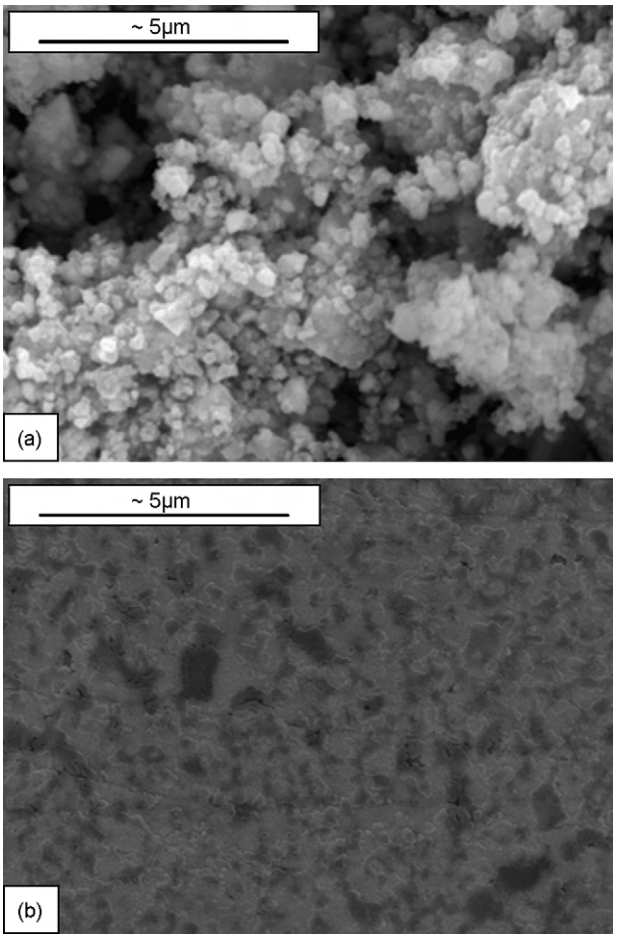

Fig. 5. Scanning electron microscope images of 4TaN + TaC + 14Si system: (a) after milling, (b) before combustion synthesis, and (c) after combustion synthesis.

The abrupt increase in the shrinkage displacement at the ignition temperature is due to the increase in density resulting from the change in the molar volume associated with the formation of $5TaSi_2$–SiC–Si_3N_4 from the reactants (TaN, TaC and Si) and the consolidation of the product.

Vickers hardness measurements were conducted on the polished sections of the $5TaSi_2$–SiC–Si_3N_4 composite using a load of 1 kg and dwell time of 15 s. The calculated hardness value, based

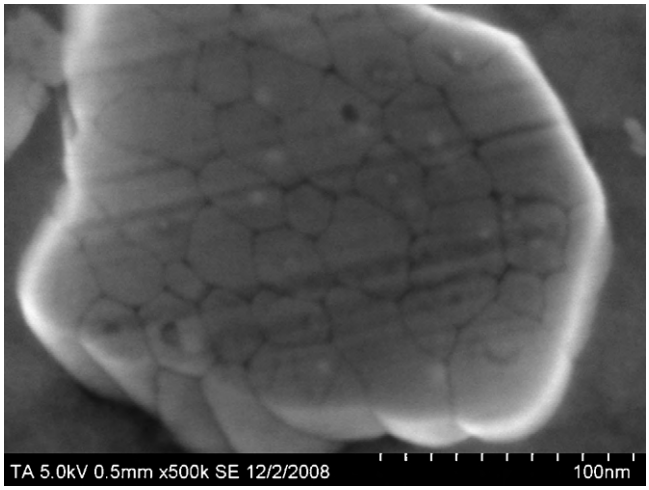

Fig. 6. FE-SEM image of $5TaSi_2$–SiC–Si_3N_4 composite sintered at 1420 °C.

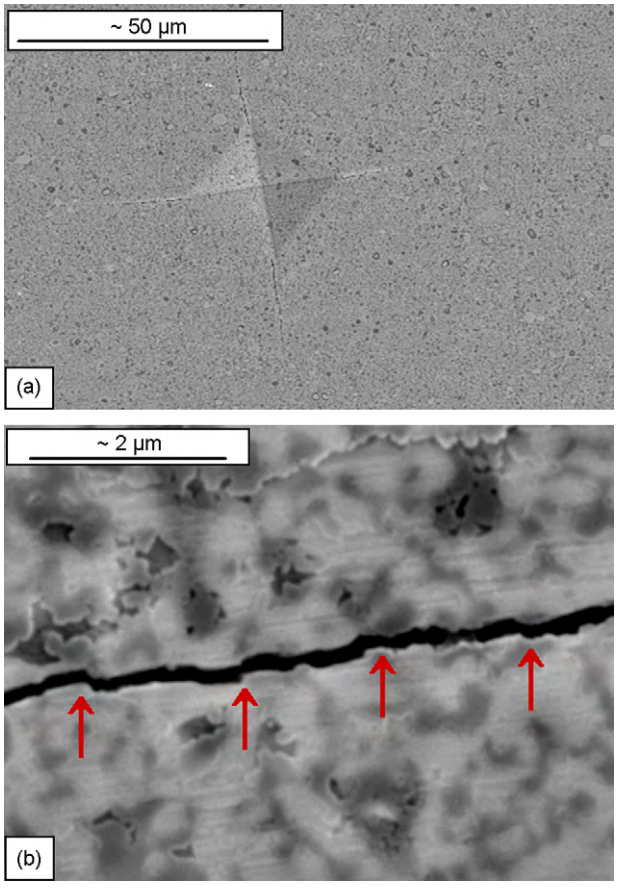

Fig. 7. (a) Vickers hardness indentation and (b) median crack propagating of $5TaSi_2$–SiC–Si_3N_4 composite.

on the average of five measurements, of the $5TaSi_2$–SiC–Si_3N_4 composite is 1250 kg/mm^2. Indentations with large enough loads produced median cracks around the indent. The length of these cracks permits the estimation of the fracture toughness of the materials by means of the expression [19]:

$$K_{IC} = 0.204\left(\frac{c}{a}\right)^{-3/2} H_v a^{1/2}$$

where c is the trace length of the crack measured from the center of the indentation, a is one half of the average length of the two indent diagonals, and H_v is the hardness. The calculated fracture toughness value for the $5TaSi_2$–SiC–Si_3N_4 composite is about 4 MPa m$^{1/2}$ As in the case of the hardness value, the toughness value is the average of five measurements. The hardness and fracture toughness of $TaSi_2$ were reported to be 908 kg/mm^2 and 3.7 MPa m$^{1/2}$, respectively [20]. The hardness and fracture toughness of $5TaSi_2$–SiC–Si_3N_4 composite are higher than those of monolithic $TaSi_2$ because hard phases of SiC and Si_3N_4 are added and crack deflects at second phase of SiC or Si_3N_4.

A typical indentation pattern for the $5TaSi_2$–SiC–Si_3N_4 composite is shown in Fig. 7. Typically, one to three additional cracks were observed to propagate from the indentation corner. A higher magnification view of the indentation median crack in the composite is shown in Fig. 7b. This shows the crack propagates deflectively (↑).

4. Summary

Using the high-frequency induction-heated combustion method, the simultaneous synthesis and densification of a nanostructured $5TaSi_2$–SiC–Si_3N_4 composite was accomplished using mechanically activated powders of TaN, TaC and Si. Complete synthesis and densification can be achieved in one step within 1 min. The relative density of the composite was 96% under an applied pressure of 60 MPa and the induced current. The average grain sizes of the $TaSi_2$, SiC and Si_3N_4 phases in the composite were about 35, 55 and 72 nm, respectively. The average hardness and fracture toughness values obtained were 1250 kg/mm^2 and 4 MPa m$^{1/2}$, respectively. The mechanical properties of the composite produced in this work are higher than those of monolithic $TaSi_2$.

References

[1] A.K. Vasudevan, J.J. Petrovic, J. Mater. Sci. Eng. A 155 (1992) 259–265.
[2] G.J. Fan, M.X. Quan, Z.Q. Hu, J. Eckert, L. Schulz, Scripta Mater. 41 (1999) 1147–1151.
[3] G. Sauthoff, Intermetallics, VCH Publishers, New York, 1995.
[4] Y. Ohya, M.J. Hoffmann, G. Petzow, J. Mater. Sci. Lett. 12 (1993) 149–152.
[5] B.W. Lin, T. Iseki, Br. Ceram. Trans. J. 91 (1992) 1–5.
[6] Y. Ohya, M.J. Hoffmann, G. Petzow, J. Am. Ceram. Soc. 75 (1992) 2479–2483.
[7] S.K. Bhaumik, C. Divakar, A.K. Singh, G.S. Upadhyaya, J. Mater. Sci. Eng. A 279 (2000) 275–281.
[8] D.K. Jang, R. Abbaschian, Kor. J. Mater. Res. 9 (1999) 92–98.
[9] H. Zhang, P. Chen, M. Wang, X. Liu, Rare Met. 21 (2002) 304–307.
[10] D.Y. Oh, H.C. Kim, J.K. Yoon, I.J. Shon, J. Alloys Compd. 395 (2005) 174–180.
[11] W. Dressler, R. Riedel, Int. J. Refract. Met. Hard Mater. 15 (1997) 13–47.
[12] S.P. Taguchi, S. Ribeiro, J. Mater. Process. Technol. 147 (2004) 336–342.
[13] T. Murakami, S. Sasaki, K. Ichikawa, A. Kitahara, Intermetallics 9 (2001) 621–628.
[14] K. Kurokawa, M. Ube, H. Takahashi, H. Takahashi, J. Phys. IV France (2000) 10–16.
[15] S. Berger, R. Porat, R. Rosen, Prog. Mater. Sci. 42 (1997) 311–320.
[16] D.Y. Oh, H.C. Kim, J.K. Yoon, I.J. Shon, J. Alloys Compd. 386 (2005) 270–275.
[17] I.J. Shon, S.C. Kim, B.S. Lee, B.R. Kim:, Electron. Mater. Lett. 5 (2009) 19–23.
[18] C. Suryanarayana, M. Grant Norton, X-ray Diffraction: A Practical Approach, Plenum Press, 1998, p. 213.
[19] K. Niihara, R. Morena, D.P.H. Hasselman, J. Mater. Sci. Lett. 1 (1982) 12–16.
[20] I.Y. Ko, J.H. Park, K.S. Nam, I.J. Shon, J. Ceram. Process. Res. 11 (2010) 69–73.